# Supporting Information

# Enhanced Photo-enzyme $CO_2$ Reduction Using PEI-Modified TPDE/$SF_N$-FE Photoenzyme Composite Catalysts

*Lin Zhang* [a, b, †], *Feng Xue* [a, †], *Shengxin Zhang* [a, b], *Qingyang Ye* [a, b], *Xinyuan Tang* [a, b*] *Liang Zhou* [c*]

[a] *Nanjing Institute of Environmental Sciences, Ministry of Ecology and Environment of the People's Republic of China, Nanjing 210042, China*

[b] *Nanjing Guohuan Environmental Research Institute Co., Ltd, Nanjing 210042, China*

[c] *School of Resources and Environmental Engineering, East China University of Science and Technology, 130 Meilong Road, Shanghai 200237, China*

[†] *These authors contribute to the work equally.*

**Text S1 Materials and chemicals**

1,3,5-Triformylresorcinol (TP) ($C_9H_6O_6$, 97.0%), n-Butanol ($C_4H_{10}O$, 99.5%), Hexadecyl Trimethyl Ammonium Bromide (CTAB) ($C_{19}H_{42}BrN$, AR), Ethanol ($C_2H_6O$, AR), L-Ascorbic Acid ($C_6H_8O_6$, AR), 2,2'-Bipyridine ($C_{10}H_8N_2$, AR), Tetraethyl Orthosilicate (TEOS) ($(C_2H_5O)_4Si$, 98.0%), Phosphate-Buffered Saline (PBS) (100 mM), and 1,2,3,4,5-Pentamethylcyclopentadienyl ($C_{10}H_{16}$, 95.0%) were purchased from Shanghai McLean Biochemical Science and Technology Co. N,N-Dimethylacetamide ($C_4H_9NO$, AR), 2,6-Diaminoanthraquinone (DAAQ) ($C_{14}H_{10}N_2O_2$, 96%), Mesitylene (Mes) ($C_9H_{12}$, 97.0%), 1,4-Dioxane (Diox) ($C_4H_8O_2$, AR), Cyclohexane ($C_6H_{12}$, 99.5%), and Acetic Acid (AcOH) ($CH_3COOH$, AR) were purchased from Shanghai Myriad Biochemistry Technology Co. Polyetherimide (PEI) ($C_{202}H_{505}N_{1013}$, 99.0%) and γ-Aminopropyltriethoxysilane (APTES) ($C_9H_{23}NO_3Si$, 98.0%) were purchased from Hangzhou Dacheng Biotechnology Co. Formate Dehydrogenase (FDH) (0.2 units/mg protein) and Urea ($CH_4N_2O$, 99.0%) were purchased from Shanghai Chuangsai Science and Technology Co. Rhodium(III) Chloride Trihydrate ($RuCl_3 \cdot 3H_2O$, 98.0%) was purchased from Shanghai BiDe Pharmaceutical Technology Co.

**Text S2 Preparation of TPDQ**

Weigh 0.3 mmol (0.0504 g) of 1,3,5-Triformylresorcinol (TP) and 0.36 mmol (0.0856 g) of 2,6-Diaminoanthraquinone (DAAQ). Transfer both to a 25 mL hydrothermal kettle. Add 15 mL of a 1:1 mixed solvent (Mes: Diox) and sonicate to achieve a homogeneous dispersion. Then, add 2.5 mL of 6 M acetic acid (AcOH) aqueous solution and sonicate again to ensure homogeneity. Freeze the hydrothermal kettle rapidly at 77 K using liquid nitrogen and degas with three freeze-pump-thaw cycles. Seal the kettle and heat at 120 °C for 72 hours. After cooling, wash the resulting solid with methanol five times, then dry and grind it under a vacuum at 80 °C. The final red powder is designated as TPDQ.

**Text S3 Preparation of silica nanoflowers (SF)**

Place 1.0 g of CTAB and 1.0 g of n-butanol into a 100 mL round-bottom flask. Add 30.0 g of a 0.4 M urea solution, and stir the mixture in a water bath at 25 °C while heating gently. Gradually add 12.0 g of cyclohexane along the flask wall to minimize frothing. Then, slowly introduce 2.0 g of TEOS and continue stirring at 25 °C for 30 minutes. Maintain stirring in a water bath at 70 °C for 20 hours. After cooling, wash the resulting white solid three times with ethanol and water. Collect the

precipitate by centrifugation, then dry the solids in an oven. Calcine the dried material in a tube furnace under air at 550 °C for 5 hours. After cooling, collect the final white powder, designated as SF.

**Text S4 Preparation of FITC-Labeled $SF_N$-FE (SF-FE)**

Dissolve 10 mg of FDH in 10 mL of PBS buffer, then add 5 mg of EDC and 2.5 mg of NHS, and stir for 2 hours. Add 100 μg of FITC and stir under dark conditions for 5 hours. Remove unreacted FITC, NHS, and EDC by dialysis (MWCO: 8 kDa) over 48 hours, replacing deionized water every 6 hours. Freeze-dry the solution to obtain FITC-labeled FDH, stored at -20 °C. Replace FDH with FITC-labeled FDH in the $SF_N$-FE preparation method to obtain FITC-labeled $SF_N$-FE (SF-FE).

**Text S5 Preparation of M ($Cp^*Rh(bpy)H_2O]^{2+}$)**

Disperse 105 mg of $RhCl_3 \cdot 3H_2O$ in 20 mL of methanol to form a red suspension. Add 65 μL of 1,2,3,4,5-pentamethylcyclopentadiene to the suspension, then reflux the mixture at room temperature for 12 hours. Transfer the solution to a pre-weighed beaker. While stirring in a fume hood, add 125 mg of 2,2'-bipyridine and 10 mL of petroleum ether, resulting in the formation of an orange precipitate. Allow the mixture to air dry for several hours. Collect and weigh the precipitate, then dissolve it in deionized water to prepare a 20 mM suspension. Label the suspension as Mbpy and store it at 4 °C in a refrigerator, protected from light.

**Text S6 Characterization**

The composition and crystal structure of the photocatalysts were characterized by X-ray diffraction (XRD) spectroscopy using a Rigaku D/max 2550 VB/PC X-ray diffractometer. The micromorphology of the materials was analyzed by transmission electron microscopy (TEM, JEOL JEM 1400), while the elemental composition was determined by X-ray photoelectron spectroscopy (XPS, Perkin-Elmer PHI 5000C ESCA). Fourier-transform infrared (FTIR) spectroscopy was performed using a Shimadzu IRTracer-100 (Japan). Electrochemical measurements were carried out on a Zahner Zennium Pro electrochemical workstation. A Pt electrode and a saturated calomel electrode were employed as the counter electrode and reference electrode, respectively. Photocurrent and Mott-Schottky tests were conducted in 0.5 M $Na_2SO_4$ electrolyte, with a 300 W xenon lamp equipped with a 420 nm filter for the photocurrent measurements. Electrochemical impedance spectroscopy (EIS) was performed in the frequency range of $1 \times 10^6$ Hz to 1 Hz with an AC amplitude of 20 mV. Laser confocal microscopy was performed using a Leica Stellaris 5 (Germany)

with an excitation wavelength of 635 nm, and both three-dimensional and planar fluorescence distributions were obtained. $N_2$ adsorption-desorption isotherms were measured at 77 K using a fully automated surface area and porosity analyzer (ASAP 2010, Micromeritics Instrument, Norcross, GA, USA) to determine the Brunauer-Emmett-Teller (BET) surface area. The absorbance and bandgap of the samples were measured using a UV-vis diffuse reflectance spectrometer (UV-vis DRS, Shimadzu UV-2450, Japan) with $BaSO_4$ as the blank reference. The optical bandgap (Eg) was calculated using equation (1):

$$(\alpha - h\nu)/n = B(h\nu - Eg) \quad (1)$$

Where α is the adsorption coefficient, h is Planck's constant, ν is the optical frequency, B is a constant, and Eg is the corresponding bandgap. Where n factor is determined by the nature of the electron jump, usually n = 1/2 for direct bandgap jumps and n = 2 for indirect bandgap jumps. In this work, the value of n is equal to 1/2 due to the nature of direct leaps in TPDQ and TPDE.

Thermogravimetric analysis was performed using a Netzsch STA 449F3 instrument (Germany) under a nitrogen atmosphere with a heating rate of 10 °C $min^{-1}$. Solid-state $^{13}C$ NMR spectra were acquired on a Bruker Avance III 500 MHz spectrometer (Switzerland) operating at a resonance frequency of 500 MHz, providing structural and dynamic information on the sample. Elemental composition analysis was conducted using an Agilent 5800 ICP-OES system (USA) to determine the catalyst's metal content and distribution. SERS measurements were carried out on a Renishaw inVia-Reflex confocal Raman microscope (UK) with a 785 nm laser excitation source. Laser confocal microscopy was performed using a Leica Stellaris 5 system (Germany) with an excitation wavelength of 635 nm, and both three-dimensional and planar fluorescence distributions were obtained.

**Text S7 Loading capacity of FDH**

The FDH loading capacity was determined by measuring the protein content of the enzyme solution, using Bradford assay, before and after adsorption. The Bradford reagent was prepared by first dissolving 100 mg of Coomassie brilliant blue G-250 powder in 50 mL of 95% ethanol, then mixing this with 100 mL of orthophosphoric acid. The solution was subsequently diluted to 1L with deionized water. Finally, the solution was vacuum-filtered and stored protected from light. To determine the FDH loading capacity, 20 μL samples of the FDH solution were withdrawn at the beginning and at the end of the adsorption test. The samples were mixed with 180 μL

of Bradford reagent and left for 5 min. The absorbance of the solutions was measured at 595 nm using UV spectrophotometer. To calculate the protein concentration in the samples, the readings were compared against a standard calibration chart, determined by measuring the absorbance of serial dilutions of known concentrations of the enzyme. The adsorption capacity, based on protein concentration, was then determined using equation (2):

$$\text{Loading ratio of FDH (\%)} = (C_0 - C_1)/C_0 \#(2)$$

Where $C_0$ is the FDH concentration in the system before the reaction and $C_1$ is the FDH concentration in the system at the end of the reaction.

**Text S8 Activity of immobilized FDH**

The activity of immobilized FDH for $CO_2$ hydrogenation were determined by a spectroscopic method based on the drop in concentration of the NADH. For activity assay, 1.0 g $NaHCO_3$ and 5.0 mg β-NADH were mixed properly in 10 mL PBS buffer. For the activity assay, a solution of 1.0 g $NaHCO_3$ and 5.0 mg β-NADH was prepared in a 10 mL PBS buffer, and subsequently subjected to rigorous agitation to ensure full dissolution. Following thorough stirring and mixing, the sample was filtered. The absorbance of NADH at 340nm was measured, and the concentration was calculated as $C_0$ according to the standard curve established by the concentration of NADH and the resulting absorption. Then, 3mg of the loaded enzyme material was added, and the reaction was continued for 1 hour. The sample was then filtered once more. The absorbance of NADH at 340nm was measured, and the concentration of $C_1$ was calculated. The recovered activity of immobilized FDH was calculated using equation (3):

$$\text{Specific activity of the FDH} = (C_0 - C_1)\cdot V/(h\cdot m_{FDH}) \#(3)$$

Where V represents the reaction volume, h denotes the reaction time, and $m_{FDH}$ is the abbreviation for the amount of enzyme contained in the loading material.

**Text S9 Procedure for photocatalytic NADH regeneration**

A 50 mL double-walled glass circulating water stirring device was used to prepare 20 mL of 100 mM PBS solution, maintaining a reaction temperature of 50 °C. To simulate the dissolved state of $CO_2$, 1.45 g of $NaHCO_3$ was added to the PBS solution. The reaction mixture included 3 mg of an enzyme-free composite catalyst, 0.5 mL of 20 mM L-Ascorbic Acid (AA) as a sacrificial agent, 0.5 mL of an electronic mediator (Mbpy), and 20 mg of the coenzyme nicotinamide adenine dinucleotide ($NAD^+$). The system was irradiated with a 420 nm xenon lamp. Initially,

the reaction was conducted in the dark for 30 minutes to allow for adsorption, followed by illumination to drive the reaction. Upon completion, the samples were filtered through a 0.22 μm filter, and the concentration of NAD(P)H in the solution was monitored using UV-Vis spectroscopy at 340 nm.

**Text S10 Rotating disc electrode (RDE) experiment**

Ag/AgCl and Pt were used as reference and counter electrodes, respectively. A glassy carbon disc with a diameter of 5 mm was used as the disc electrode and a rotating disc electrode was used as the working electrode. The working electrodes were obtained by the drop-casting method. Generally, 5 mg of catalyst was added into a mixture of 950 μL ethanol, 50 μL Nafion solution, and 20 μL water, and then ultrasonicated for about 30 min to make the catalyst dispersed uniformly. The suspension was then taken and dropped onto the disc electrode, which was mechanically polished and ultrasonically cleaned. The surface loading of the material was 0.25 mg/cm$^2$. All electrochemical evaluations were carried out at 25 °C with $N_2$ aeration for 30 min in a solution of $NAD^+$, $NaHCO_3$, $NAD^+$ + $NaHCO_3$. The tests were performed at rotational speeds of 400, 625, 900, 1225, and 1600 rpm throughout the measurements. Linear scanning voltammetry (LSV) tests were performed at a scanning speed of 10.0 mV/s with test potentials ranging from -1.0 V to 0.2 V.

The average number of electrons (n) involved in the overall $CO_2$ reduction process was calculated by the following equation:

$$j^{-1} = jk^{-1} + B^{-1}\omega^{-1/2} \quad (4)$$

$$B = 0.620nFC_0D_0^{2/3}v^{-1/6} \quad (5)$$

Where j is the current density (mA cm$^{-2}$), jk is the kinetic current density (mA cm$^{-2}$), ω is the rotational velocity (rpm), F is Faraday's constant (96485 C mol$^{-1}$), ν is the kinetic viscosity of water (0.01cm$^2$ s$^{-1}$). $C_0$ is the volume concentration of $NAD^+$ and $NaHCO_3$ in water ($NAD^+$ = 1×10$^{-3}$ mol cm$^{-3}$, $NaHCO_3$ = 1×10$^{-3}$ mol cm$^{-3}$), $D_0$ is the diffusion concentration of $NAD^+$ and $NaHCO_3$ in water ($NAD^+$ = 0.6×10$^{-5}$ cm$^2$ s$^{-1}$, $NaHCO_3$ = 0.9×10$^{-5}$ cm$^2$ s$^{-1}$).

**Text S11 Rotating disc electrode (RDE) experiment**

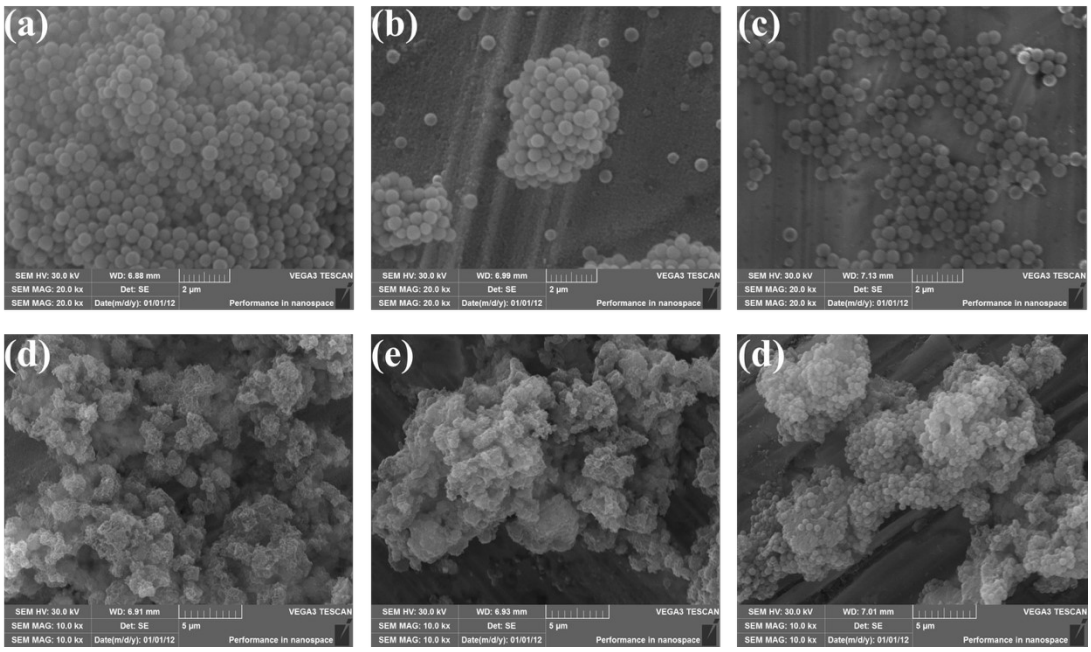


**Fig. S1**. SEM images of (a) SF, (b) $SF_N$, (c) $SF_N$-FE, (d) TPDQ, (e) TPDE and TPDE/$SF_N$-FE.

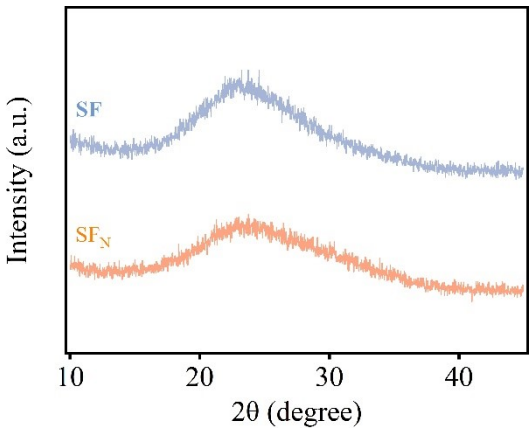


**Fig. S2**. XRD patterns of SF, $SF_N$ and $SF_N$-FE.

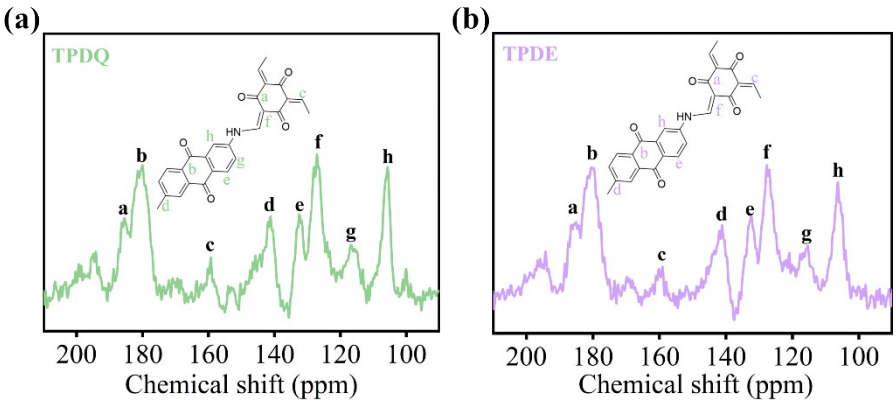


**Fig. S3**. $^{13}C$ solid-state NMR spectra of TPDQ and TPDE.

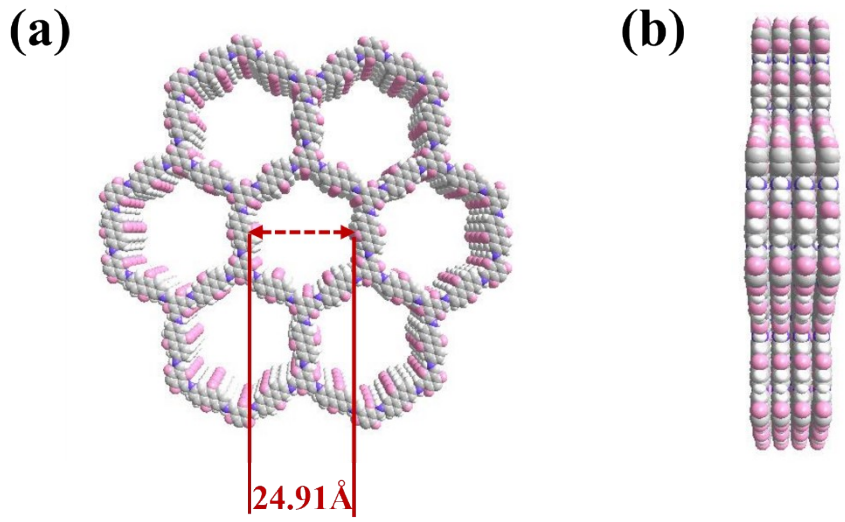


**Fig. S4**. Schematic diagram of TPDQ 3D structure simulation.

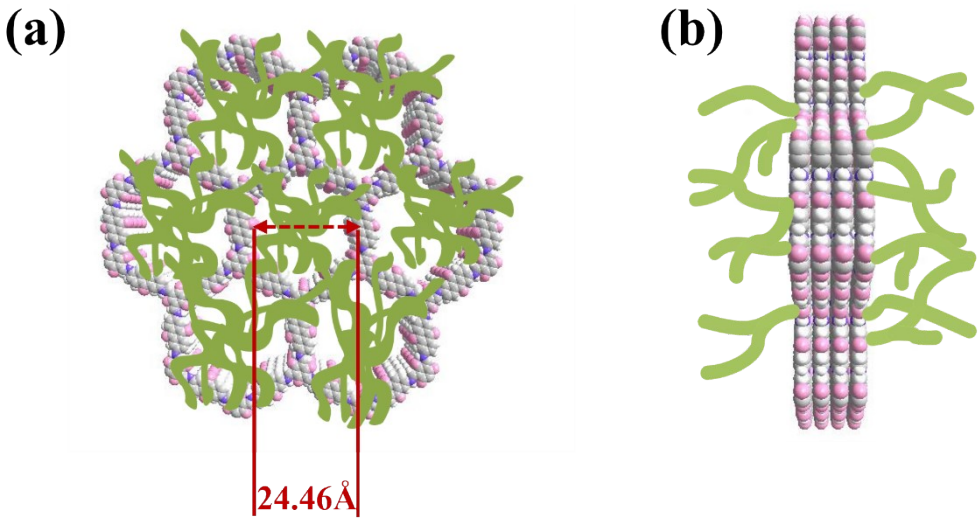


**Fig. S5**. Schematic diagram of TPDE 3D structure simulation.

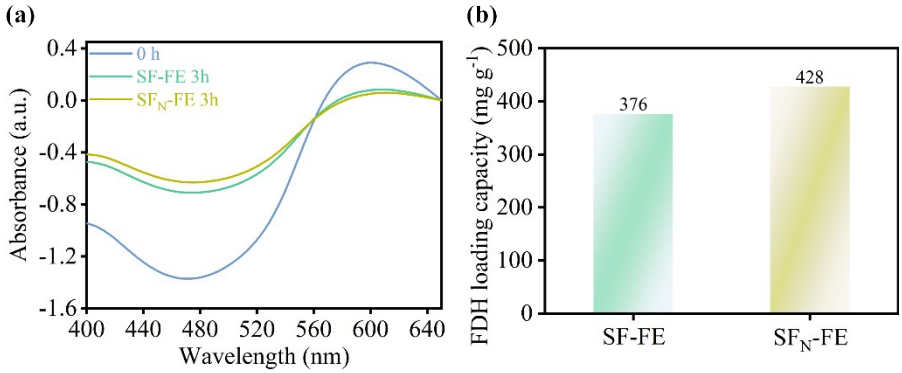


**Fig. S6.** (a) UV-vis adsorption spectra of SF-FE and $SF_N$-FE; (b) FDH loading amount of SF-FE and $SF_N$-FE.

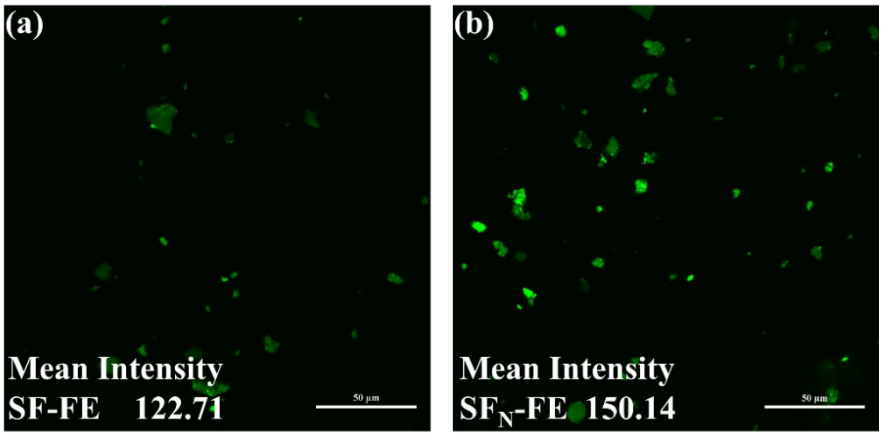


**Fig. S7.** CLSM images of the FITC-tagged (a) SF-FE and (b) $SF_N$-FE.

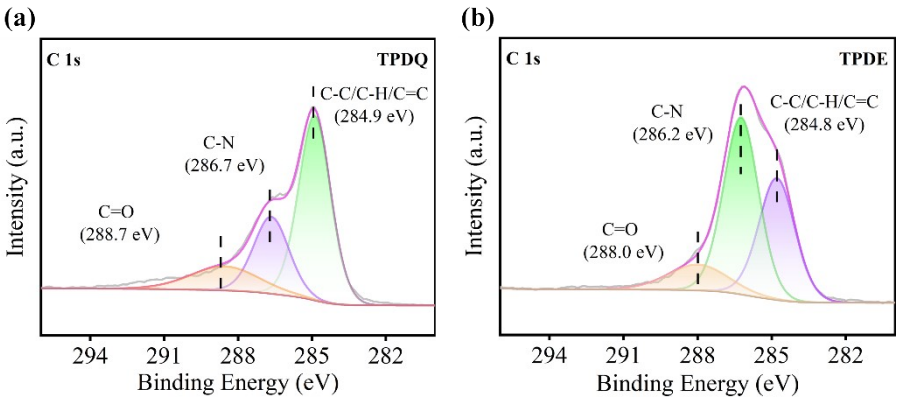


**Fig. S8**. C 1s XPS spectra of (a) TPDQ and (b) TPDE.

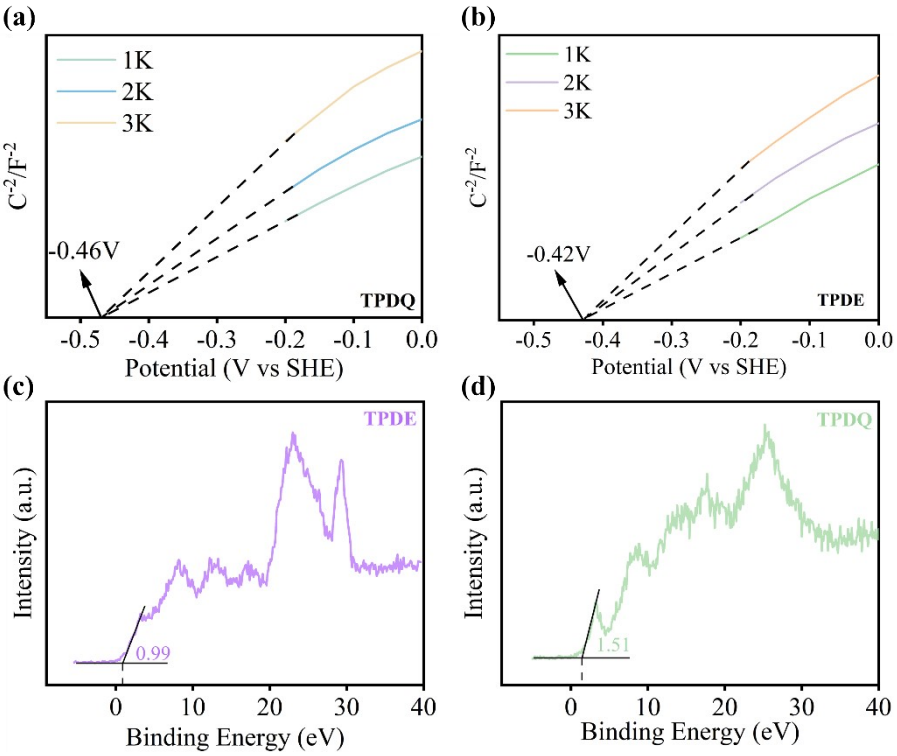


**Fig. S9**. Mott-Schottky plots of (a) TPDQ and (b) TPDE; XPS valence spectra of (c) TPDQ and (d) TPDE.

**Table S1**. The BET surface area and pore structure data of TPDQ and TPDE.

| Samples | $S_{BET}$[a] ($m^2 g^{-1}$) | $S_{micro}$[b] ($m^2 g^{-1}$) | $V_{total}$[c] ($cm^3 g^{-1}$) | $V_{micro}$[d] ($cm^3 g^{-1}$) | Pore size (nm) |
|---|---|---|---|---|---|
| **TPDQ** | 200 | 55 | 0.51 | 0.029 | 15 |
| **TPDE** | 52 | 6 | 0.33 | 0.003 | 34 |

a The $S_{BET}$ was calculated by using the BET model.

b The $S_{micro}$ (d < 2 nm) was calculated by using the t-plot method.

c The $V_{total}$ was calculated at $P/P_0 = 0.99$.

d The $V_{micro}$ (d < 2 nm) was calculated by using a t-plot model.

**Table S2.** Statistical comparison of formic acid yield efficiency from $CO_2$ reduction by different photo-enzyme system.

| Photocatalyst, sacrificial agent, $NAD^+$, light source | FDH/U | M/mg | HCOOH /μmol $U^{-1}$ $mg^{-1}$ $h^{-1}$ | Ref. |
|---|---|---|---|---|
| 0.625 mg/mL of Ce/TCPP-UiO-66-NH2, 5 mM of TEOA, 1 mM of $NAD^+$, Xe Lamp, Cut 420 nm | 6 | 1.53 | 3.37 | [1] |
| 0.5 mg/mL of PCN@TA/PEI-Rh, 400 mM of TEOA, 5 mM of $NAD^+$, LED, 405 nm | 16 | 2.88 | 0.091 | [2] |
| 1.5 mg/mL of ATCN-DSCN, 15 w/v% of TEOA, 1 mM $NAD^+$, Xe Lamp, Cut 420 nm | 10 | 0.115 | 0.083 | [3] |
| 1.2 mg/mL of ATCN-CN, 100 mM of TEOA, 1 mM of $NAD^+$, Xe Lamp, Cut 420 nm | 2 | 0.51 | 0.323 | [4] |
| 1 mg/mL of $TDM_{0.15}$, 15% v/v of TEOA, 5 mM of $NAD^+$, Xe Lamp, Cut 420 nm | 1 | 15.3 | 3.25 | [5] |
| 3 mg/mL of 10 %In-CdS@ZIF-8&FDH, 0.3 M of TEOA, 1 mM of $NAD^+$, Xe lamp, Cut 420 nm | 15.84 | 0.408 | 9.78 | [6] |
| 10 mg of PDI/CN, 15 wt% of TEOA, 0.1 mM of $NAD^+$, Xe lamp, AM1.5 | 3 | 25.725 | 0.164 | [7] |
| 3 mg of TPDE/$SF_N$-FE, 0.5 mM of AA, 1 mg/mL of $NAD^+$, Xe lamp, Cut 420 nm | 1.5 | 1.029 | 10.85 | This work |

* P=HCOOH/μmol $U^{-1}$ $g^{-1}$ $h^{-1}$ is calculated using the following formula:

$$P = \frac{A}{B * C * t}$$

A was the amount of HCOOH, the unit is μmol, B was the amount of FDH, the unit is U, C was the amount of Rh, the unit is g, t was time, the unit is hour. $NAD^+$ acts as a recyclable cofactor, while L-ascorbic acid is a relatively inexpensive sacrificial electron donor. In contrast, the Rh-based mediator represents a more cost-sensitive component, and formate formation in the coupled system is mainly associated with the FDH-mediated pathway. Therefore, the Rh- and enzyme-normalized productivity

provides an additional measure of the resource efficiency of the photo-enzyme cascade.

## Reference

1. H. Gao, L. Luan, J. Cai, X. Ji, H. Yu, Y. Huang, Chem. Eng. J., 2024, 479, 147720
2. Y. Cheng, J. Shi, Y. Wu, X. Wang, Y. Sun, Z. Cai, Y. Chen, Z. Jiang, Research, 2021, 2021, 8175709
3. J. Meng, Y. Tian, C. Li, X. Lin, Z. Wang, L. Sun, Y. Zhou, J. Li, N. Yang, Y. Zong, F. Li, Y. Cao, H. Song, Catal. Sci. Technol., 2019, 9, 1911-1921
4. Q. Liao, R. Gao, F. Sun, R. Chong, Z. Meng, W. Liu, J. Clean. Prod., 2024, 436, 140661
5. H. Zheng, Z. Huang, P. Wei, Y. Lin, Y. Cao, X. Zhang, B. Zhou, C. Peng, ACS Sustainable Chem. Eng., 2025, 13, 4078-4092
6. J. Zhou, X. Tian, S. Yu, Z. Zhao, Y. Ji, U. Schwanebrg, B. Chen, T. Tan, Z. Cui, M. Wang, Chem. Eng. Sci., 2024, 285, 119613
7. P. Zhang, J. Hu, Y. Shen, X. Yang, J. Qu, F. Du, W. Sun, C. Li, ACS Appl. Mater. Interfaces 2021, 13, 46650-46658